Analytical Letters

ISSN: (Print) (Online) Journal homepage: https://www.tandfonline.com/loi/lanl20

Characterization of Bacteria Inducing Chronic Sinusitis Using Surface-Enhanced Raman Spectroscopy (SERS) with Multivariate Data Analysis

Rana Zaki Abdul Bari, Haq Nawaz, Muhammad Irfan Majeed, Nosheen Rashid, Muhammad Tahir, Hafiz Mahmood ul Hasan, Shazra Ishtiaq, Nimra Sadaf, Ali Raza, Anam Zulfiqar, Aziz ur Rehman & Muhammad Shahid

To cite this article: Rana Zaki Abdul Bari, Haq Nawaz, Muhammad Irfan Majeed, Nosheen Rashid, Muhammad Tahir, Hafiz Mahmood ul Hasan, Shazra Ishtiaq, Nimra Sadaf, Ali Raza, Anam Zulfiqar, Aziz ur Rehman & Muhammad Shahid (2023) Characterization of Bacteria Inducing Chronic Sinusitis Using Surface-Enhanced Raman Spectroscopy (SERS) with Multivariate Data Analysis, Analytical Letters, 56:8, 1351-1365, DOI: 10.1080/00032719.2022.2130349

To link to this article: https://doi.org/10.1080/00032719.2022.2130349

ANALYTICAL LETTERS
2023, VOL. 56, NO. 8, 1351–1365
https://doi.org/10.1080/00032719.2022.2130349

Taylor & Francis
Taylor & Francis Group

RAMAN

Characterization of Bacteria Inducing Chronic Sinusitis Using Surface-Enhanced Raman Spectroscopy (SERS) with Multivariate Data Analysis

Rana Zaki Abdul Bari[a], Haq Nawaz[a], Muhammad Irfan Majeed[a], Nosheen Rashid[b], Muhammad Tahir[a], Hafiz Mahmood ul Hasan[a], Shazra Ishtiaq[a], Nimra Sadaf[a], Ali Raza[a], Anam Zulfiqar[a], Aziz ur Rehman[c], and Muhammad Shahid[d]

[a]Department of Chemistry, University of Agriculture Faisalabad, Faisalabad, Pakistan; [b]Department of Chemistry, University of Education, Faisalabad, Pakistan; [c]Department of Chemistry, Government College University Lahore, Lahore, Pakistan; [d]Department of Biochemistry, University of Agriculture Faisalabad, Faisalabad, Pakistan

ABSTRACT

Sinusitis is the inflammation of the mucous membrane lining the paranasal sinuses, and if symptoms and signs of sinusitis last for more than 12 weeks, it is categorized to be chronic. In this work, the characterization of cell mass/pellets of three bacterial strains, *Klebsiella pneumoniae, Enterococcus faecalis,* and *Staphylococcus aureus*, which cause chronic sinusitis, was performed by surface-enhanced Raman Spectroscopy (SERS). These bacteria that induce chronic sinusitis were cultured and isolated from the nasal swab of a patient and identified by the 16S rRNA sequences performed on isolated strains. The bacteria were characterized by their SERS characteristics, showing the potential of this method. SERS features at 594, 822, 831, 944, 1030, 1170, and 1268 cm^{-1} were the differentiating features of these bacteria. Moreover, multivariate data analysis was performed by principal component analysis (PCA) and partial least squares—discriminate analysis (PLS-DA) and shown to be suitable for the differentiation and classification of these bacteria. The spectral features were characterized by PCA for classification. PLS-DA was applied for further validation of differentiation which provides accuracy and sensitivity above 90% in all of the models. The area under curve (AUC) was near 1 for all PLS-DA models.

ARTICLE HISTORY
Received 5 August 2022
Accepted 25 September 2022

KEYWORDS
Bacterial strains; partial least squares—discriminate analysis (PLS-DA); principal component analysis (PCA); sinusitis; surface-enhanced Raman spectroscopy (SERS)

Introduction

Sinusitis is the inflammation of the mucous membrane lining the paranasal sinuses. If symptoms and signs of sinusitis last for more than 12 weeks, it is categorized as chronic (Clement et al. 1998). According to national population surveys and insurance reimbursement claims, sinusitis is one of the most prevalent health issues in the United States (DeMuri and Wald 2012). The development of bacterial sinusitis is caused by a

CONTACT Haq Nawaz haqchemist@yahoo.com; Muhammad Irfan Majeed irfan.majeed@uaf.edu.pk Department of Chemistry, University of Agriculture Faisalabad, Faisalabad 38000, Pakistan; Muhammad Shahid mshahiduaf@yahoo.com Department of Biochemistry, University of Agriculture Faisalabad, Faisalabad 38000, Pakistan.

Supplemental data for this article can be accessed online at https://doi.org/10.1080/00032719.2022.2130349

Table 1. Details of the bacteria samples.

Sample name	Bacterial strains
E1	*Enterococcus faecalis*
E2	*Enterococcus faecalis*
E3	*Enterococcus faecalis*
K1	*Klebsiella pneumoniae*
K2	*Klebsiella pneumoniae*
K3	*Klebsiella pneumoniae*
S1	*Staphylococcus aureus*
S2	*Staphylococcus aureus*
S3	*Staphylococcus aureus*

blockage or inflammation of the osteomeatal complex (OMC), which prevents adequate mucociliary clearance. The OMC is an integral anatomic region where the drainage sections of the paranasal sinuses confluence (Brook 2007). Symptoms of chronic bacterial sinusitis include facial pain, nasal obstruction, nasal secretion, and headache, as well as other symptoms of the upper respiratory tract (Melen 1994). The bacteria that cause chronic sinusitis include *Enterococcus faecalis* (*E. faecalis*) (Pandak et al. 2011), *Klebsiella pneumoniae* (*K. pneumoniae*) (Shahid et al. 2021), and *Staphylococcus aureus* (*S. aureus*) (Brook 2007) (Table 1).

The identification and detection of microorganisms are important in water, biodefense, food, water safety, and human health care (Granger et al. 2016). Bacterial characterization has traditionally been accomplished by laborious and time-consuming procedures including plating and culture tests (Wang et al. 2012; Pahlow et al. 2015), visual microscopic investigation, biochemical responses, and physiological function evaluation (Nelson, Manoharan, and Sperry 1992). Alternative approaches such as enzyme-linked immunosorbent assays (Zhu et al. 2016) and flow cytometry (Gunasekera, Attfield, and Veal 2000). Spectroscopic techniques such as fluorescence (Giana et al. 2003), infrared (IR) (Maquelin et al. 2003), and Raman spectroscopy (Akanny et al. 2020) are increasingly utilized to reduce the analysis time. In case of IR, due to its significant absorbance caused by water in the infrared range, its use remains challenging (Efrima and Zeiri 2009).

For rapid characterization, noninvasive, and qualitative analysis, Raman spectroscopy is widely recognized as a valuable analytical tool. It is potentially a technique of choice because it is simple to use, inexpensive, rapid, and provides high-quality information about the composition and interactions of biomolecules within microorganisms (Tahir et al. 2020). Raman spectroscopy methods are appropriate to study these biological systems. However, the utilization of concentrated samples is necessary due to the inherently weak Raman signal (Le Ru and Etchegoin 2008). Nanostructured metal surfaces are used in surface-enhanced Raman spectroscopy (SERS) to increase the signal. Indeed, analytes display enhanced signals when interacting with the metal framework, potentially lowering their detection limit to the single molecule level (Stiles et al. 2008).

In a previous study, SERS was employed to analyze centrifuged serum of hepatitis B patients. Principal component analysis (PCA) and partial least squares—discriminate analysis (PLS-DA) were employed to characterize the samples with favorable accuracy, precision, and sensitivity (Bari et al. 2022).

In this study, SERS was employed for the characterization of three bacteria which cause chronic sinusitis: *Enterococcus faecalis* (*E. faecalis*), *Klebsiella pneumoniae* (*K.*

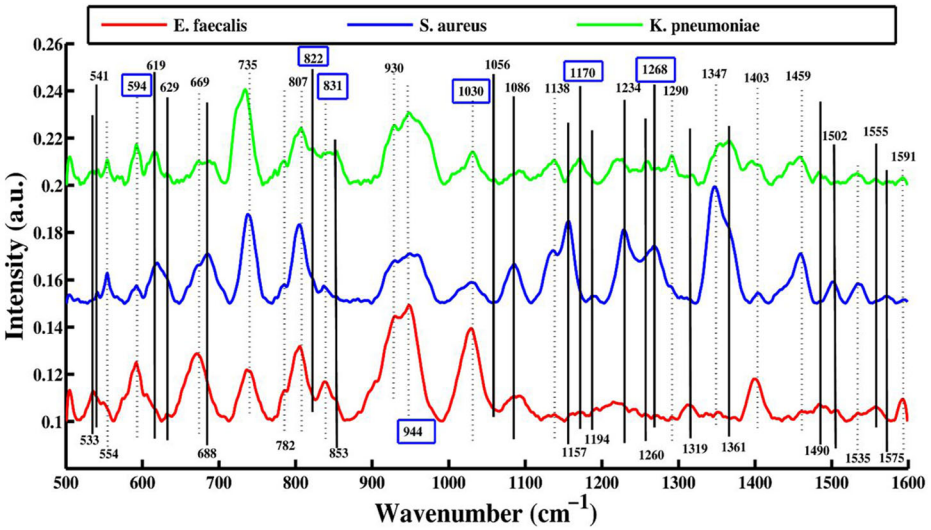

Figure 1. Mean spectra of surface-enhanced Raman spectroscopy (SERS) of *Klebsiella pneumonia* (green), *Enterococcus faecalis* (red), and *Staphylococcus aureus* (blue).

pneumoniae), and *Staphylococcus aureus* (*S. aureus*). The classification and differentiation of the SERS data sets were performed by principal component analysis (PCA) and partial least squares—discriminate analysis (PLS-DA).

Materials and methodology

Preparation of silver nanoparticles

The chemical reduction was employed for the preparation of the silver nanoparticles (AgNPs) SERS substrate. Trisodium citrate was used as a reducing and stabilizing agent. First, 300 mL of distilled water were mixed with 0.0085 g of silver nitrate, heated with continuous stirring, and 10 mL of 10% trisodium citrate were introduced. The volume of this solution was decreased to 100 mL by heating to produce grey nanoparticles.

Scanning and transmission electron microscopies (SEM, TEM) (JEOL, JSM-7500F) were employed to characterize the morphology and size of the AgNPs (Kashif et al. 2020). Utilizing ImageJ software, an electron micrograph was examined, demonstrating that the AgNPs were oval-shaped and possessed an average size of 65 × 45 nm, as shown in Supplementary Figure S1.

Sample preparation

A sampling of chronic sinusitis patients was done at the ENT OPD Allied Hospital, Faisalabad. The nasal swabs were cultured on blood, cystine lactose electrolyte deficient (CLED), and MacConkey agar and incubated for 24 to 48 hours at 37 °C in the presence of 5% CO_2. Different colonies were selected and cultured again. For characterization and identification, 16S rRNA sequences were performed on isolated strains. Identified strains were preserved in glycerol stock for further use.

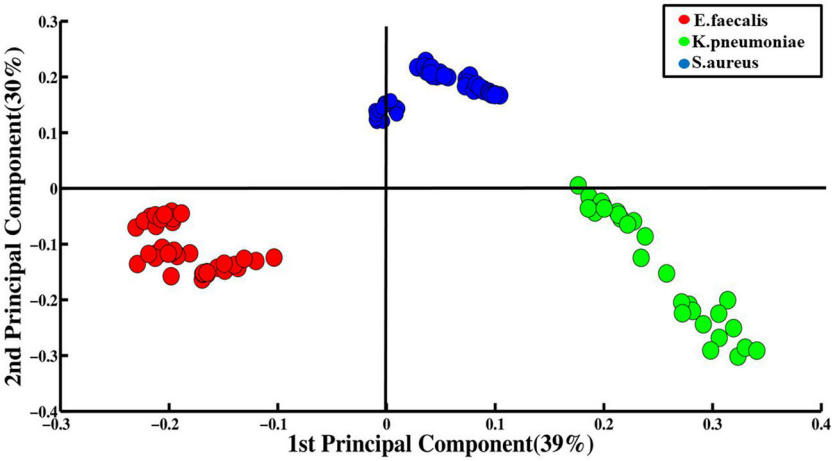

Figure 2. Principal component analysis (PCA) scatter plot of the SERS spectra of *Klebsiella pneumonia, Enterococcus faecalis,* and *Staphylococcus aureus.*

Acquisition of SERS spectra

Three samples of *E. faecalis*, 3 samples of *K. pneumoniae*, and 3 samples of *S. aureus* were employed in this work. The SERS spectra were acquired using a Peak Seeker Pro-785 (Agiltron, USA) spectrometer. The excitation source is a diode laser operating at 785 nm. Moreover, 50 μl of each bacterial sample was treated with 50 μl of AgNPs to obtain the SERS spectra with incubation for 30 minutes which were the optimized conditions (Chen et al. 2019). The sample volume of the aluminum slide is filled with 100 µl of the incubation mixture (Kashif et al. 2020). The SERS-spectra were collected using a 40×/0.6(N.A) lens with a 10-second integration time. A total of 15 spectra were obtained for each sample as shown in Supplementary Figures S2–S10.

SERS preprocessing

MatLab version 7.8 was used to preprocess the SERS spectra (Nawaz et al. 2017) by vector normalization, substrate removal, baseline correction, and smoothing. Smoothing and vector normalization were performed by Savitzky–Golay and rubber band correction, respectively.

Data analysis

The SERS features of bacteria were analyzed by comparing mean spectra and peak assignments were made by consultation with the literature as shown in Table 2. PCA and PLS-DA were employed for the classification and differentiation of the bacteria. In order to decrease the dimensionality of the data while maintaining its variability, PCA is a mathematical unsupervised technique that involves the conversion of potentially correlated variables into a smaller number of uncorrelated variables, known as principal components (PCs). This approach provides qualitative analysis with considering inter- and intra-sample variability.

PLS-DA is a supervised model which helps to discover the underlying relationships between variables and is designed to process large numbers of highly collinear elements.

Table 2. Peak assignments of SERS spectra of the bacteria causing chronic sinusitis.

Wavenumber (cm^{-1})	Assignment	References
533	S–S str., COC glycosidic ring def.	Paret et al. 2010
541	δ (C2-Cl-Ol vibration)	Özbalci et al. 2013
554	C–S–S–C	Çulha et al.
594	Phosphatidylinositol	Movasaghi, Rehman, and Rehman 2007
619	Phenylalanine	De Gelder et al. 2007a
629	d(NCO) Tyr	Sockalingum et al. 1999
669	Guanine	Paret et al. 2010
688	Low frequency in pyranoid ring	Synytsya et al. 2003
735	Adenine	Zeiri et al. 2004
782	Phosphodiester stretching	Williams and Edwards 1994
807	n(PO_2), n(CC) ring breathing (DNA)	Sockalingum et al. 1999
822	tyrosine	De Gelder et al. 2007b
831	Out-of-plane ring breathing in DNA	Talari et al. 2015
853	(C–C–O–C–O)	Özbalci et al. 2013
930	a-helix (protein) C–O–C	Goeller and Riley 2007
944	Lipid components	Neugebauer et al. 2007
1030	n(CC) aromatic ring	Edwards et al. 1995
1056	Carbohydrates, C–C, C–O, –C–OH def	Laucks et al. 2005
1086	C-O-C asymmetric stretching in aliphatic esters	Neugebauer et al. 2007
1138	C–C (Unsaturated fatty acids in lipids)	Schuster, Urlaub, and Gapes 2000
1157	C–C stretch (v2) vibrations of the polyene chain of carotenoids/ xanthomonadin1	Schulz, Baranska, and Baranski 2005
1170	Tyrosine	López-Díez and Goodacre 2004
1194	Tyrosine	López-Díez and Goodacre 2004
1234	Amide III	Nishijima et al. 2004
1260	Amide III	Paret et al. 2010
1268	Amide III	Neugebauer et al. 2007
1290	Amide III	Nishijima et al. 2004
1319	d(CH_2), in-plane d(OH)	Edwards et al. 1995
1347	(C-O-H bending vibration)	Galat 1980
1459	CH_2 scissoring,	De Gussem et al. 2005
1361	C–H bending (proteins)	Laucks et al. 2005
1403	COO^- symmetric stretching	Laucks et al. 2005
1490	Adenine	Wu et al. 2001
1502	Amide II	Sockalingum et al. 1999
1535	N-acetyl-related (Amide II)	Neugebauer et al. 2007
1575	Amide II	Edwards et al. 1995
1555	Amide II	Neugebauer et al. 2007
1591	n(C = C) aromatic	Sockalingum et al. 1999

This technique allows the identification of the predictive features of data sets which help to classify samples. This approach provides qualitative and quantitative analysis while maintaining inter and intra-sample variability better than PCA. In addition, this classification model gives different quantitative parameters of differentiation and classification in terms of accuracy, precision, and validity (Lê et al. 2018; Ai et al. 2021; Batool et al. 2021).

Results and discussion

Mean SERS spectra

Figure 1 shows the mean SERS spectra of *Klebsiella pneumonia, Enterococcus faecalis,* and *Staphylococcus aureus*. The peaks in the blue boxes are characteristic which are

differentiating features in all strains and include 594, 822, 831, 944, 1030, 1170, and 1268 cm^{-1}. The biochemical features present in all strains are represented by dotted lines and include 554, 594, 669, 735, 782, 807, 831, 930, 944, 1030, 1138, 1290, 1347, 1403, 1459, 1535, and 1591 cm^{-1}.The SERS enhanced bands which depict dissimilarities are denoted by solid lines and include 533, 541, 619, 629, 688, 822, 853, 1056, 1086, 1157, 1170, 1194, 1234, 1260, 1268, 1319, 1361, 1490, 1502, 1555, and 1575 cm^{-1}.

In the spectral region between 500 and 800 cm^{-1}, SERS features may be observed at 533 cm^{-1}(S–S, COC glycosidic ring) which is only present in *E. faecalis and K. pneumoniae* (Paret et al. 2010). The SERS bands at 541 $cm^{-1}\delta$ (C2-Cl-Ol vibration), 619 cm^{-1} (phenylalanine), and 688 cm^{-1} (guanine) are only present in *S. aureus* and *K. pneumoniae*. The peak at 629 cm^{-1} (NCO) is only observed in *K. pneumoniae* and *E. faecalis*.

The region from 800 to 1250 cm^{-1} also exhibits SERS bands at 822 cm^{-1} (tyrosine), 853 cm^{-1}(C–C–O–C–O), 1056 cm^{-1} (C–C, C–O, –C–OH carbohydrates), and 1170 cm^{-1} (tyrosine) only in *K. pneumoniae*. The 1086 cm^{-1} (C-O-C asymmetric stretching in aliphatic esters) 1157 cm^{-1} (C–C) peaks are in *S. aureus* and *E. faecalis*, while 1194 cm^{-1} (tyrosine) and 1234 cm^{-1} (amide III) are only observed in *S. aureus* (Nishijima et al. 2004).

Differences in the SERS features were also observed between 1250 and 1600 cm^{-1} that include 1260 and 1268 cm^{-1} that are Amide III peaks. These peaks are present in *E. faecalis* and *K. pneumoniae* at 1260 and at 1268 cm^{-1} in *S. aureus*. Similarly, SERS features at 1361 cm^{-1} (C–H bending of proteins) are only in *K. pneumoniae*. The 1502 cm^{-1} (Amide II) peak is only observed in *E. faecalis* and *S. aureus*. The Amide II SERS bands are at 1555 cm^{-1} in *K. pneumoniae* and *E. faecalis* and 1575 cm^{-1} in *S. aureus* (Edwards et al. 1995). Other peaks are at 1319 cm^{-1} ($d(CH_2)$ in-plane d(OH) and 1490 cm^{-1} (adenine) present in *K. pneumoniae* and *E. faecalis*.

Furthermore, the SERS peaks present in all of the bacteria but with intensity differences include 554 cm^{-1} (C–S–S–C bonds) which has similar intensities in *S. aureus* and *K. pneumoniae* but reduced intensity in *E. faecalis*. The phosphatidylinositol band at 594 cm^{-1} is more intense in *E. faecalis* than *K. pneumoniae* but lower in *S. aureus*. The SERS peak at 669 cm^{-1} is due to guanine and is more intense in *E. faecalis* than *S. aureus* and less intense in *K. pneumoniae*. The peak at 735 cm^{-1} is due to adenine and is more intense in *K. pneumoniae* and *S. aureus* than *E. faecalis* (Zeiri et al. 2004). The phosphodiester stretch and $n(PO_2)$ n(CC) ring breathing of DNA are at 782 and 807 cm^{-1}, respectively. These SERS bands have similar intensity in all strains of the bacteria.

Furthermore, the 831 cm^{-1} peak (out-of-plane ring breathing in DNA) is more intense in *E. faecalis* than *S. aureus* but less intense in *K. pneumoniae*. The 930 cm^{-1} (α-helix proteins) and 944 cm^{-1} (lipids) are more intense in *E. faecalis* and *K. pneumoniae* than in *S. aureus* and may be used to discriminate the bacteria. SERS bands at 1030 and 1591 cm^{-1} (aromatic ring) are more intense in *E. faecalis* than *K. pneumoniae* but less in *S. aureus*. The unsaturated fatty acid of the lipid peak at 1138 cm^{-1} is less intense in *K. pneumoniae* than *S. aureus* and lowest in *E. faecalis*. A peak at 1290 cm^{-1} (Amide III) is less intense in *S. aureus* than *K. pneumoniae* but lowest in *E. faecalis*. The peaks at 1347 and 1459 cm^{-1} are more intense in *S. aureus* than *K. pneumoniae* (De Gussem et al. 2005) but lowest in *E. faecalis*, perhaps due to the C-O-H bending

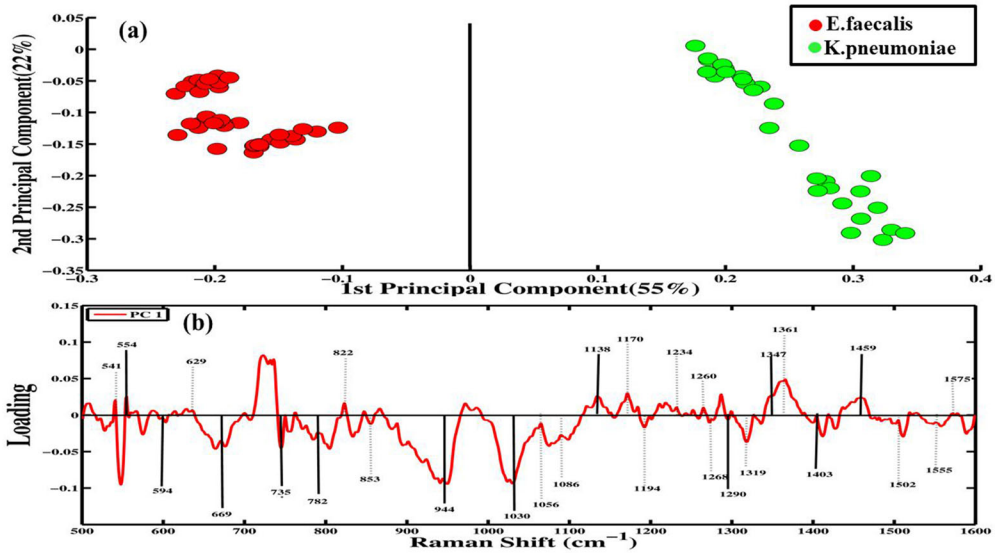

Figure 3. (a) Principal component analysis (PCA) scatter plot of the SERS spectra of *Enterococcus faecalis* (red) and *Klebsiella pneumoniae* (green). (b) PCA loading of SERS spectra between *Enterococcus faecalis* and *Klebsiella pneumoniae*.

vibration of oligosaccharides. The peak at 1403 cm^{-1} (COO^- symmetric stretch) is more intense in *E. faecalis* than *S. aureus* but lowest in *K. pneumoniae*. Moreover, 1535 cm^{-1} is an Amide II SERS band that is more intense in *S. aureus* than *K. pneumoniae* but lowest in *E. faecalis*.

Principal component analysis (PCA)

SERS data sets of three types of bacteria were subjected to PCA, a statistical method, to identify variance and differentiation in the distinct datasets, as well as the reasons for this differentiation. PCA operates by lowering the dimensionality of data while leaving variability unchanged (Liu et al. 2013). Figure 2 represents a scatter plot of SERS spectra of *Klebsiella pneumonia, Enterococcus faecalis,* and *Staphylococcus aureus* showing their classification. *E. faecalis* is shown in red clustered in the negative side of the abscissa (*x*-axis). The positive abscissa (PC-1) represents *K. pneumoniae* in green while *S. aureus* is in blue positive to the *y*-axis (PC-2). The SERS spectra of *K. pneumoniae* are grouped on the positive abscissa (PC-1) in green while *S. aureus* strains in blue are present on the positive *y*-axis. Principal component analysis (PCA) provides good classification and differentiation among the bacteria. PC-1 and PC-2 express variance values of 39% and 30%, respectively.

Figure 3a shows the scatter plot of PCA of *E. faecalis* and *K. pneumoniae* where PC-1 explains 55% of the variance and PC-2 22%. The red points represent *E. faecalis* which are present on the negative abscissa (PC-1) and the green *K. pneumoniae* on the positive abscissa (PC-1). The scatter plot of PCA shows that the strains are different with good classification by SERS.

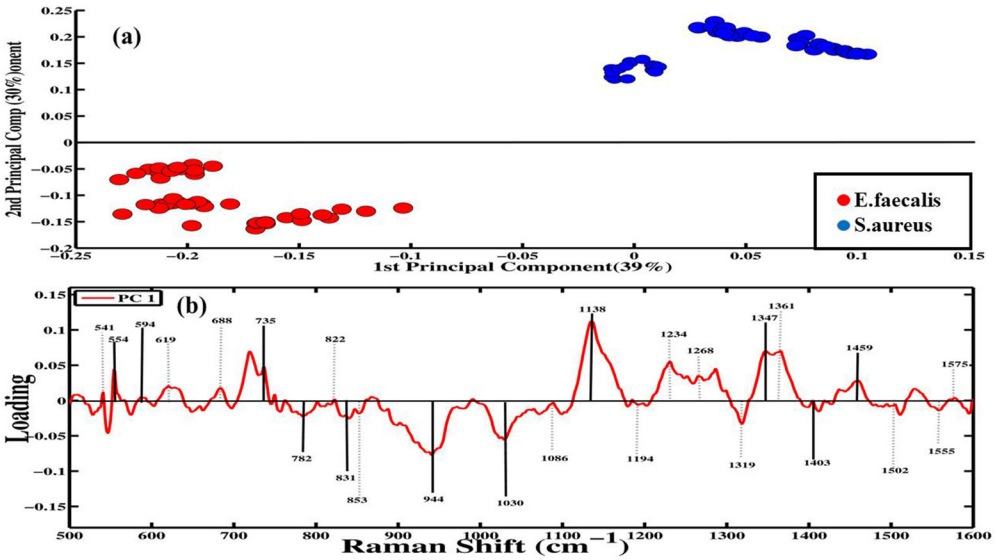

Figure 4. (a) Principal component analysis (PCA) scatter plot of SERS spectra of *Enterococcus faecalis* (red) and *Staphylococcus aureus* (blue). (b) PCA loading of SERS spectra between *Enterococcus faecalis* and *Staphylococcus aureus*.

Figure 3b shows the PCA-loadings (PC-1) of these bacteria. The negative loadings include 594, 669, 735, 782, 853, 944, 1030, 1056, 1086, 1194, 1268, 1290, 1319, 1403, 1502, and 1555 cm^{-1} are due to *E. faecalis* present on the negative abscissa (PC-1). The peaks at 541, 554, 629, 822, 1138, 1170, 1234, 1260, 1347, 1361, 1459, and 1575 cm^{-1} are positive loading associated with *K. pneumoniae* and are located on the positive abscissa (PC-1). Moreover, the PCA loadings are related to SERS features in the mean plot of the bacteria (Figure 1).

Figure 4a shows the PCA scatter plot for the SERS spectra of *E. faecalis* and *S. aureus*. The red points are due to *E. faecalis* located on the negative ordinate (PC-2) and blue due to *S. aureus* SERS measurements clustered toward the positive ordinate (PC-2). Figure 4a shows differentiation of the SERS data sets of these bacteria. The 39% variance and 30% variance in the SERS spectra are shown by PC1 and PC2, respectively.

Figure 4b presents PCA-loadings of *E. faecalis* and *S. aureus*. The positive loadings, which include 541, 554, 594, 619, 688, 735, 822, 1138, 1234, 1268, 1347, 1361, 1459, and 1575 cm^{-1}, are due to *S. aureus* grouped on the positive ordinate (PC-2). The negative loadings at 782, 831, 853, 944, 1030, 1086, 1194, 1319, 1403, 1502, and 1555 cm^{-1} are due to SERS datasets of *E. faecalis* clustered on the negative ordinate (PC-2). The PCA-loadings of *E. faecalis* and *S. aureus* match the distinct SERS features in the mean plot which confirms these results.

Figure 5a shows the PCA-scatter plot of SERS enhanced datasets of *K. pneumoniae* and *S. aureus*. The SERS data sets of *K. pneumoniae* are in green on the negative portion of the *y*-axis, while blue represents the *S. aureus* spectra on the positive ordinate (PC-2). Each spectrum is displayed by one point. The PCA scatter plot distinguishes the bacterial strains. Variability values of 53% and 29% are provided by PC1 and PC2, respectively.

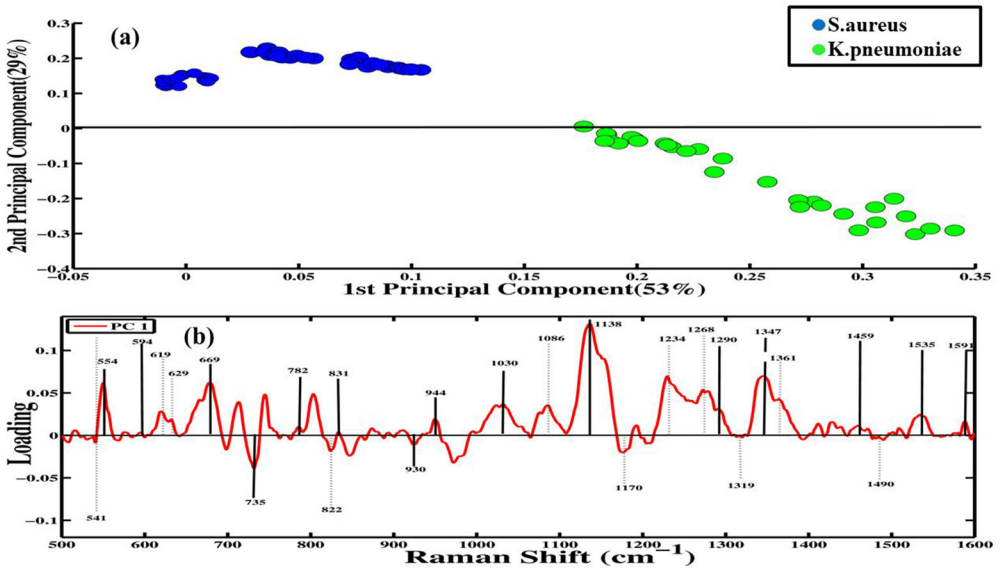

Figure 5. (a) Principal component analysis (PCA) scatter plot of SERS spectra of *Klebsiella pneumoniae* (green) and *Staphylococcus aureus* (blue). (b) PCA loading of SERS spectra between *Klebsiella pneumoniae* and *Staphylococcus aureus*.

Figure 5b shows the PCA-loadings of SERS spectra of these bacteria: the positive loadings are due to *S. aureus* which is clustered in the positive region of PC-2 in the scatter plot. These loadings include 554, 594, 619, 629, 669, 782, 831, 944, 1030, 1086, 1138, 1234, 1268, 1290, 1347, 1361, 1459, 1535, and 1591 cm^{-1}. The negative-loadings include 735, 822, 930, 1170, 1319, and 1490 cm^{-1} that are due to *K. pneumoniae* on the negative portion of PC-2 in the plot. The PCA-loadings are matched with distinct SERS features in the mean plot (Figure 1).

Figures 3b, 4b, and 5b show pair-wise PCA loadings by comparison of the SERS data sets. The PCA loadings are employed to show significant differentiating features indicating biochemical differences in the bacteria. In PCA loading figures, the changes due to one bacterium strain are present in the positive region and other in the negative region as peaks. These biochemical changes shown in the PCA loadings are matched with distinct SERS features in the mean spectrum (Figure 1).

Partial least squares—discriminate analysis (PLS-DA)

The PLS-DA model was employed to differentiate the SERS signals of three bacteria that cause sinusitis using pair-wise comparison. The model was calibrated using training data. Monte Carlo cross-validation was employed to select latent variables based upon the Bayes theorem. For this purpose, the calibration and validation data were 60% and 40%, respectively, and the number of latent variables employed was 5.

Figure 6a shows the PLS-DA score plot of SERS data sets of *E. faecalis* (red) on the positive portion of *y*-axis while negative region of the *y*-axis of score plot shows the *K. pneumoniae* data set (green). The score plot of this classification model provides good differentiation of the SERS spectra of these bacteria with a specificity of 98%, an

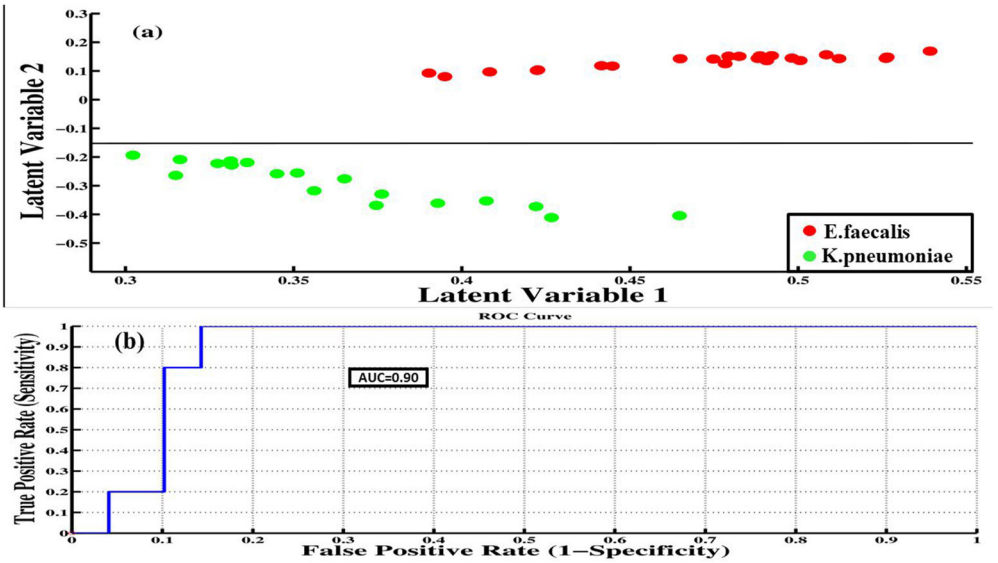

Figure 6. (a) Partial least squares—discriminate analysis (PLS-DA) scatter diagram of SERS spectra of *Enterococcus faecalis* (red) and *Klebsiella pneumoniae* (green). (b) Receiver operating characteristic curve (ROC) of PLS-DA for SERS spectra of *Enterococcus faecalis* (red) and *Klebsiella pneumoniae* (green).

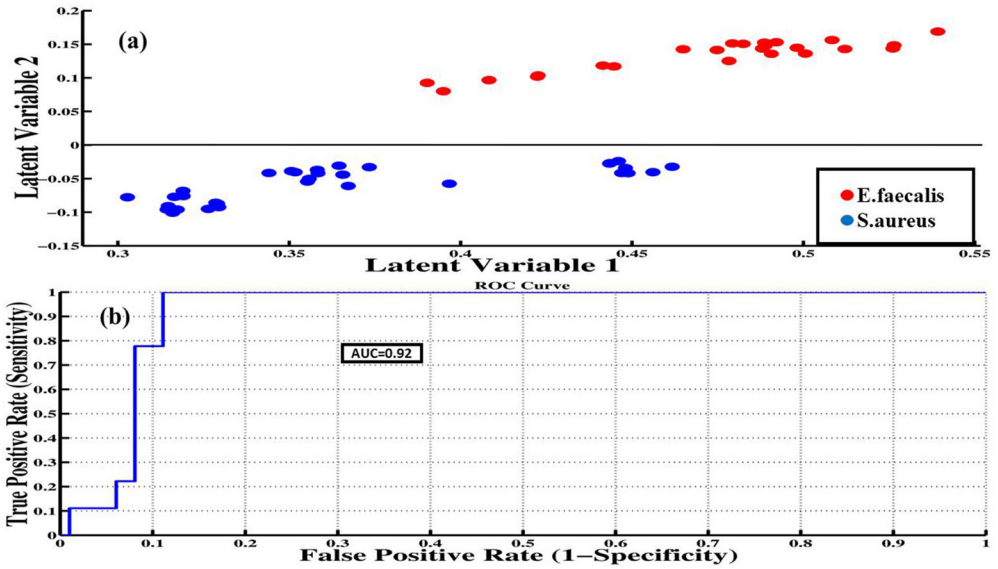

Figure 7. (a) Partial least squares—discriminate analysis (PLS-DA) scatter diagram of SERS spectra of *Enterococcus faecalis* (red) and *Staphylococcus aureus* (blue). (b) Receiver operating characteristic curve (ROC) of PLS-DA for SERS spectra of *Enterococcus faecalis* (red) and *Staphylococcus aureus* (blue).

accuracy of 97%, and a sensitivity of 97%. Figure 6b shows the receiver operating characteristic curve (ROC) of the PLS-DA model with an area under curve (AUC) value equal to 0.90.

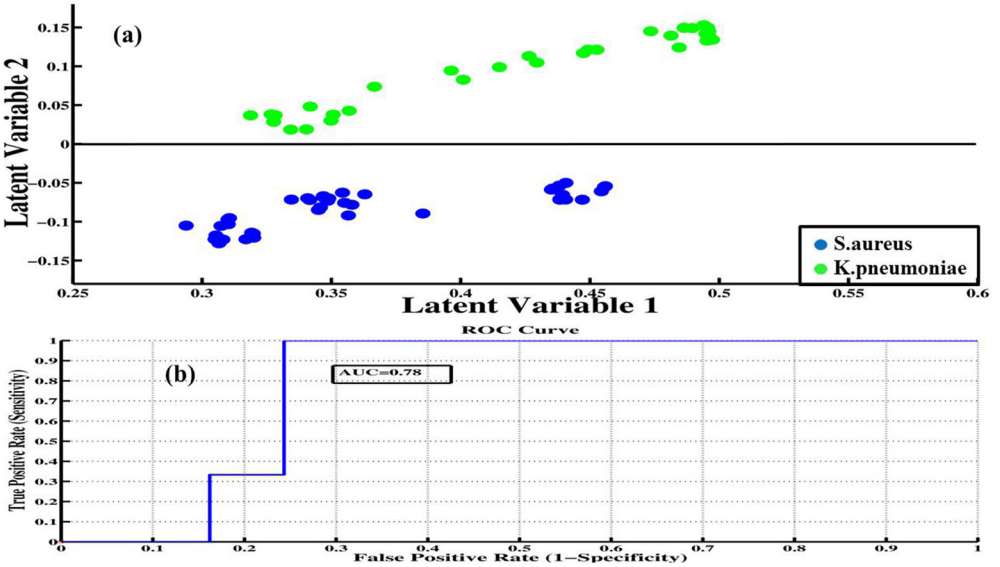

Figure 8. (a) Partial least squares—discriminate analysis (PLS-DA) scatter diagram of SERS spectra of *Klebsiella pneumoniae* (green) and *Staphylococcus aureus* (blue). (b) Receiver operating characteristic curve (ROC) of PLS-DA for SERS spectra of *Klebsiella pneumoniae* (green) and *Staphylococcus aureus* (blue).

Figure 7a displays the PLS-DA score plot on which the positive side of *y*-axis is clustered with SERS spectra of *E. faecalis* (red) and negative side of *y*-axis is clustered with *S. aureus* SERS spectra (blue). The specificity was 94%, the accuracy 91%, and the sensitivity 97%. Figure 7b shows ROC curve of PLS-DA model with the area under curve equal to 0.92.

The PLS-DA model score plot of SERS spectra of *K. pneumoniae* and *S. aureus* are shown in Figure 8a. The spectra of *K. pneumoniae* clustered on the positive side are in green while the negative side of score plot shows the cluster of the *S. aureus* spectra in blue. The accuracy, specificity, and sensitivity were 96%, 97%, and 98%, respectively. The AUC value of ROC curve is 0.78 as shown in Figure 8b.

The PLS-DA model with SERS provides excellent results for the classification and differentiation of the bacteria that cause sinusitis. The cross validation of model is shown by ROC curve and accuracy of model is indicated by the value of AUC. An AUC value near zero shows that model is inaccurate, while a value near 1 indicates high accuracy. The values of AUC are near 1 in all of PLS-DA scatter diagrams of three bacteria shown as pair-wise comparisons. Therefore, the constructed PLS-DA model provides the excellent classification and differentiation of these bacteria.

Conclusions

SERS was demonstrated to provide excellent differentiation between *Klebsiella pneumonia, Enterococcus faecalis,* and *Staphylococcus aureus*, three bacteria that cause sinusitis. SERS enhanced features due to these bacteria were identified for characterization and identification. Furthermore, PCA and PLS-DA were employed for the differentiation of

the SERS spectra. Pairwise PCA was performed to compare the SERS spectral datasets of the bacteria. PLS-DA provided an AUC value near 1 for all data sets allowing the classification of the bacteria. SERS spectral features were identified for these bacteria that may be employed as markers for their identification.

Disclosure statement

The authors declare that they have no conflicts of interest.

Statement of ethical approval

It is hereby stated that all the experimental work involved in this study has been approved by the ethical committee of University of Agriculture Faisalabad, Pakistan.

ORCID

Muhammad Irfan Majeed http://orcid.org/0000-0003-0506-6060

References

Ai, J., Q. Wu, M. Battino, W. Bai, and L. Tian. 2021. Using untargeted metabolomics to profile the changes in roselle (*Hibiscus sabdariffa* L.) anthocyanins during wine fermentation. *Food Chemistry* 364:130425. doi:10.1016/j.foodchem.2021.130425.

Akanny, E., A. Bonhommé, C. Commun, A. Doleans-Jordheim, C. Farre, F. Bessueille, S. Bourgeois, and C. Bordes. 2020. Surface-enhanced Raman spectroscopy using uncoated gold nanoparticles for bacteria discrimination. *Journal of Raman Spectroscopy* 51 (4):619–29. doi:10.1002/jrs.5827.

Bari, R. Z. A., H. Nawaz, M. I. Majeed, N. Rashid, M. Iqbal, M. Akram, N. Yaqoob, S. Yousaf, A. Mushtaq, F. Almas, et al. 2022. Surface-enhanced Raman spectroscopic analysis of centrifugally filtered HBV serum samples. *Photodiagnosis and Photodynamic Therapy* 38:102808. doi:10.1016/j.pdpdt.2022.102808.

Batool, F., H. Nawaz, M. I. Majeed, N. Rashid, S. Bashir, S. Bano, F. Tahir, A. U. Haq, M. Saleem, M. Z. Nawaz, et al. 2021. Surface-enhanced Raman spectral analysis for comparison of PCR products of hepatitis B and hepatitis C. *Photodiagnosis and Photodynamic Therapy* 35: 102440. doi:10.1016/j.pdpdt.2021.102440.

Brook, I. 2007. Acute and chronic bacterial sinusitis. *Infectious Disease Clinics of North America* 21 (2):427–48, vii. doi:10.1016/j.idc.2007.02.001.

Chen, X., M. Tang, Y. Liu, J. Huang, Z. Liu, H. Tian, Y. Zheng, M. L. de la Chapelle, Y. Zhang, and W. Fu. 2019. Surface-enhanced Raman scattering method for the identification of methicillin-resistant *Staphylococcus aureus* using positively charged silver nanoparticles. *Microchimica Acta* 186 (2):1–8.

Clement, P. A., C. D. Bluestone, F. Gordts, R. P. Lusk, F. W. Otten, H. Goossens, G. K. Scadding, H. Takahashi, F. L. van Buchem, P. Van Cauwenberge, et al. 1998. Management of rhinosinusitis in children: Consensus meeting, Brussels, Belgium, September 13, 1996. *Archives of Otolaryngology-Head & Neck Surgery* 124 (1):31–4. doi:10.1001/archotol.124.1.31.

De Gelder, J., K. De Gussem, P. Vandenabeele, and L. Moens. 2007a. Reference database of Raman spectra of biological molecules. *Journal of Raman Spectroscopy* 38 (9):1133–47. doi:10.1002/jrs.1734.

De Gelder, J., K. De. Gussem, P. Vandenabeele, M. Vancanneyt, P. De Vos, and L. Moens. 2007b. Methods for extracting biochemical information from bacterial Raman spectra: Focus

on a group of structurally similar biomolecules—fatty acids. *Analytica Chimica Acta* 603 (2): 167–75. doi:10.1016/j.aca.2007.09.049.

De Gussem, K., P. Vandenabeele, A. Verbeken, and L. Moens. 2005. Raman spectroscopic study of *Lactarius* spores (Russulales, Fungi). *Spectrochimica Acta: Part A, Molecular and Biomolecular Spectroscopy* 61 (13–14):2896–908. doi:10.1016/j.saa.2004.10.038.

DeMuri, G. P, and E. R. Wald. 2012. Acute bacterial sinusitis in children. *New England Journal of Medicine* 367 (12):1128–34. doi:10.1056/NEJMcp1106638.

Edwards, H., N. Russell, R. Weinstein, and D. Wynn-Williams. 1995. Fourier transform Raman spectroscopic study of fungi. *Journal of Raman Spectroscopy* 26 (8–9)-:911–6. doi:10.1002/jrs.1250260843.

Efrima, S, and L. Zeiri. 2009. Understanding SERS of bacteria. *Journal of Raman Spectroscopy* 40 (3):277–88. doi:10.1002/jrs.2121.

Galat, A. 1980. Study of the Raman scattering and infrared absorption spectra of branched polysaccharides. *Acta Biochimica Polonica*. 27 (2):135–42.

Giana, H. E., L. Silveira, R. A. Zângaro, and M. T. T. Pacheco. 2003. Rapid identification of bacterial species by fluorescence spectroscopy and classification through principal components analysis. *Journal of Fluorescence* 13 (6):489–93. doi:10.1023/B:JOFL.0000008059.74052.3c.

Goeller, L. J, and M. R. Riley. 2007. Discrimination of bacteria and bacteriophages by Raman spectroscopy and surface-enhanced Raman spectroscopy. *Applied Spectroscopy* 61 (7):679–85. doi:10.1366/000370207781393217.

Granger, J. H., N. E. Schlotter, A. C. Crawford, and M. D. Porter. 2016. Prospects for point-of-care pathogen diagnostics using surface-enhanced Raman scattering (SERS). *Chemical Society Reviews* 45 (14):3865–82. doi:10.1039/c5cs00828j.

Gunasekera, T., P. Attfield, and D. Veal. 2000. A flow cytometry method for rapid detection and enumeration of fungal spores in the atmosphere. *Applied and Environmental Microbiology* 66 (3):1228–32. doi:10.1128/AEM.66.3.1228-1232.2000.

Kashif, M., M. I. Majeed, M. A. Hanif, and A. ur Rehman. 2020. Surface Enhanced Raman Spectroscopy of the serum samples for the diagnosis of Hepatitis C and prediction of the viral loads. *Spectrochimica Acta: Part A, Molecular and Biomolecular Spectroscopy* 242:118729. doi:10.1016/j.saa.2020.118729.

Laucks, M. L., A. Sengupta, K. Junge, E. J. Davis, and B. D. Swanson. 2005. Comparison of psychro-active arctic marine bacteria and common mesophillic bacteria using surface-enhanced Raman spectroscopy. *Applied Spectroscopy* 59 (10):1222–8. doi:10.1366/000370205774430891.

Le Ru, E, and P. Etchegoin. 2008. *Principles of surface-enhanced Raman spectroscopy: And related plasmonic effects*. UK: Elsevier.

Lê, L., M. Berge, A. Tfayli, P. Prognon, and E. Caudron. 2018. Discriminative and quantitative analysis of antineoplastic taxane drugs using a handheld Raman spectrometer. *BioMed Research International* 2018:8746729. doi:10.1155/2018/8746729.

Liu, S.-Y., R.-L. Zhang, H. Kang, Z.-J. Fan, and Z. Du. 2013. Human liver tissue metabolic profiling research on hepatitis B virus-related hepatocellular carcinoma. *World Journal of Gastroenterology* 19 (22):3423. doi:10.3748/wjg.v19.i22.3423.

López-Díez, E. C, and R. Goodacre. 2004. Characterization of microorganisms using UV resonance Raman spectroscopy and chemometrics. *Analytical Chemistry* 76 (3):585–91. doi:10.1021/ac035110d.

Maquelin, K., C. Kirschner, L.-P. Choo-Smith, N. A. Ngo-Thi, T. van Vreeswijk, M. Stämmler, H. P. Endtz, H. A. Bruining, D. Naumann, and G. J. Puppels. 2003. Prospective study of the performance of vibrational spectroscopies for rapid identification of bacterial and fungal pathogens recovered from blood cultures. *Journal of Clinical Microbiology* 41 (1):324–9. doi:10.1128/JCM.41.1.324-329.2003.

Melen, I. 1994. Chronic sinusitis: Clinical and pathophysiological aspects. *Acta Oto-Laryngologica* 114 (Suppl 515):45–8.

Movasaghi, Z., S. Rehman, and I. U. Rehman. 2007. Raman spectroscopy of biological tissues. *Applied Spectroscopy Reviews* 42 (5):493–541. doi:10.1080/05704920701551530.

Nawaz, H., N. Rashid, M. Saleem, M. Asif Hanif, M. Irfan Majeed, I. Amin, M. Iqbal, M. Rahman, O. Ibrahim, S. M. Baig, et al. 2017. Prediction of viral loads for diagnosis of Hepatitis C infection in human plasma samples using Raman spectroscopy coupled with partial least squares—regression analysis. *Journal of Raman Spectroscopy* 48 (5):697–704. doi:10.1002/jrs.5108.

Nelson, W., R. Manoharan, and J. Sperry. 1992. UV resonance Raman studies of bacteria. *Applied Spectroscopy Reviews* 27 (1):67–124. doi:10.1080/05704929208018270.

Neugebauer, U., U. Schmid, K. Baumann, W. Ziebuhr, S. Kozitskaya, V. Deckert, M. Schmitt, and J. Popp. 2007. Towards a detailed understanding of bacterial metabolism—spectroscopic characterization of *Staphylococcus epidermidis*. *Chemphyschem: A European Journal of Chemical Physics and Physical Chemistry* 8 (1):124–37. doi:10.1002/cphc.200600507.

Nishijima, K., A. Alvarez, P. Hepperly, M. Shintaku, L. Keith, D. Sato, B. Bushe, J. Armstrong, and F. Zee. 2004. Association of *Enterobacter cloacae* with rhizome root of edible ginger in Hawaii. *Plant Disease* 88 (12):1318–27. doi:10.1094/PDIS.2004.88.12.1318.

Özbalci, B., İ H. Boyaci, A. Topcu, C. Kadılar, and U. Tamer. 2013. Rapid analysis of sugars in honey by processing Raman spectrum using chemometric methods and artificial neural networks. *Food Chemistry* 136 (3–4):1444–52. doi:10.1016/j.foodchem.2012.09.064.

Pahlow, S., S. Meisel, D. Cialla-May, K. Weber, P. Rösch, and J. Popp. 2015. Isolation and identification of bacteria by means of Raman spectroscopy. *Advanced Drug Delivery Reviews* 89: 105–20. doi:10.1016/j.addr.2015.04.006.

Pandak, N., I. Pajić-Penavić, A. Sekelj, M. Tomić-Paradžik, I. Čabraja, and B. Miklaušić. 2011. Bacterial colonization or infection in chronic sinusitis. *Wiener Klinische Wochenschrift* 123 (23–24):710–3. doi:10.1007/s00508-011-0093-x.

Paret, M. L., S. K. Sharma, L. M. Green, and A. M. Alvarez. 2010. Biochemical characterization of Gram-positive and Gram-negative plant-associated bacteria with micro-Raman spectroscopy. *Applied Spectroscopy* 64 (4):433–41. doi:10.1366/000370210791114293.

Schulz, H., M. Baranska, and R. Baranski. 2005. Potential of NIR-FT-Raman spectroscopy in natural carotenoid analysis. *Biopolymers: Original Research on Biomolecules* 77 (4):212–21. doi:10.1002/bip.20215.

Schuster, K. C., E. Urlaub, and J. Gapes. 2000. Single-cell analysis of bacteria by Raman microscopy: Spectral information on the chemical composition of cells and on the heterogeneity in a culture. *Journal of Microbiological Methods* 42 (1):29–38. doi:10.1016/S0167-7012(00)00169-X.

Shahid, M., I. Naureen, M. Riaz, F. Anjum, H. Fatima, and M. A. Rafiq. 2021. Biofilm inhibition and antibacterial potential of different varieties of garlic (*Allium sativum*) against sinusitis isolates. *Dose-Response: A Publication of International Hormesis Society* 19 (4):. doi:10.1177/15593258211050491.

Sockalingum, G. D., H. Lamfarraj, A. Beljebbar, P. Pina, M. Delavenne, F. Witthuhn, P. Allouch, M. Manfait. 1999. "Vibrational spectroscopy as a probe to rapidly detect, identify, and characterize micro-organisms," *Proc. SP IE 3608, Biomedical Applications of Raman Spectroscopy*. doi:10.1117/12.345401.

Stiles, P. L., J. A. Dieringer, N. C. Shah, and R. P. Van Duyne. 2008. Surface-enhanced Raman spectroscopy. *Annual Review of Analytical Chemistry (Palo Alto, Calif.)* 1:601–26. doi:10.1146/annurev.anchem.1.031207.112814.

Synytsya, A., J. Čopıková, P. Matějka, and V. Machovič. 2003. Fourier transform Raman and infrared spectroscopy of pectins. *Carbohydrate Polymers* 54 (1):97–106. doi:10.1016/S0144-8617(03)00158-9.

Tahir, M., M. I. Majeed, H. Nawaz, S. Ali, N. Rashid, M. Kashif, I. Ashfaq, W. Ahmad, K. Ghauri, F. Sattar, et al. 2020. Raman spectroscopy for the analysis of different exo-polysaccharides produced by bacteria. *Spectrochimica Acta: Part A, Molecular and Biomolecular Spectroscopy* 237:118408. doi:10.1016/j.saa.2020.118408.

Talari, A. C. S., Z. Movasaghi, S. Rehman, and I. U. Rehman. 2015. Raman spectroscopy of biological tissues. *Applied Spectroscopy Reviews* 50 (1):46–111. doi:10.1080/05704928.2014.923902.

Wang, J., J. Gao, D. Liu, D. Han, and Z. Wang. 2012. Phenylboronic acid functionalized gold nanoparticles for highly sensitive detection of *Staphylococcus aureus*. *Nanoscale* 4 (2):451–4. doi:10.1039/c2nr11657j.

Williams, A, and H. Edwards. 1994. Fourier transform Raman spectroscopy of bacterial cell walls. *Journal of Raman Spectroscopy* 25 (7–8):673–7. doi:10.1002/jrs.1250250730.

Wu, Q., T. Hamilton, W. H. Nelson, S. Elliott, J. F. Sperry, and M. Wu. 2001. UV Raman spectral intensities of *E. coli* and other bacteria excited at 228.9, 244.0, and 248.2 nm. *Analytical Chemistry* 73 (14):3432–40. doi:10.1021/ac001268b.

Zeiri, L., B. Bronk, Y. Shabtai, J. Eichler, and S. Efrima. 2004. Surface-enhanced Raman spectroscopy as a tool for probing specific biochemical components in bacteria. *Applied Spectroscopy* 58 (1):33–40. doi:10.1366/000370204322729441.

Zhu, L., J. He, X. Cao, K. Huang, Y. Luo, and W. Xu. 2016. Development of a double-antibody sandwich ELISA for rapid detection of *Bacillus Cereus* in food. *Scientific Reports* 6 (1): 16092–10. doi:10.1038/srep16092.